Particle Identification with dE/dx (dN/dx)

F. Grancagnolo - INFN Lecce

15 January 2021

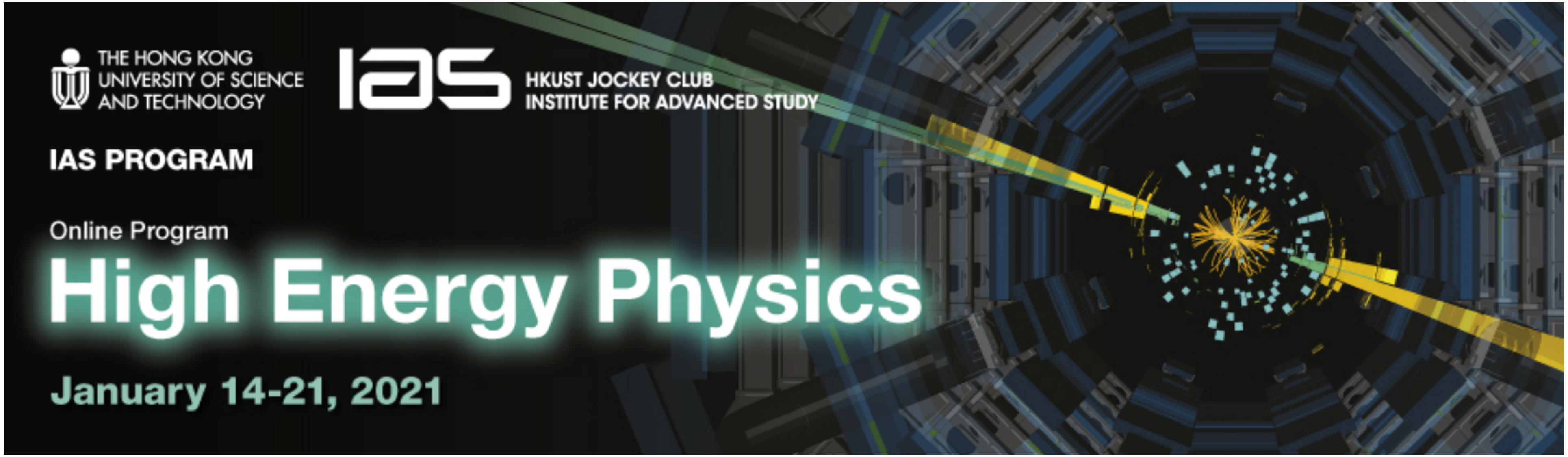

OUTLINE

- Thanks to the preceding excellent presentations, there is no need here to motivate the relevance of a **PId** system for a detector at **CEPC** and **FCCee**.
- Focus the attention exclusively to the **energy loss measurement** (**dE/dx**) and to **cluster counting** (**$dN_{cluster}$/dx**) **techniques** for **PId** in drift chambers.
  (please, do not expect exhaustive treatments of such complex arguments in 30 min)
- Describe the procedures from measurements to observables.
- Estimate the expected performance in both cases, using currently available technologies.
- List the constraining parameters which limit the expected performance.

PId techniques

$$\frac{m^2}{p^2} = \frac{1}{\gamma^2 - 1} = \frac{1-\beta^2}{\beta^2}$$

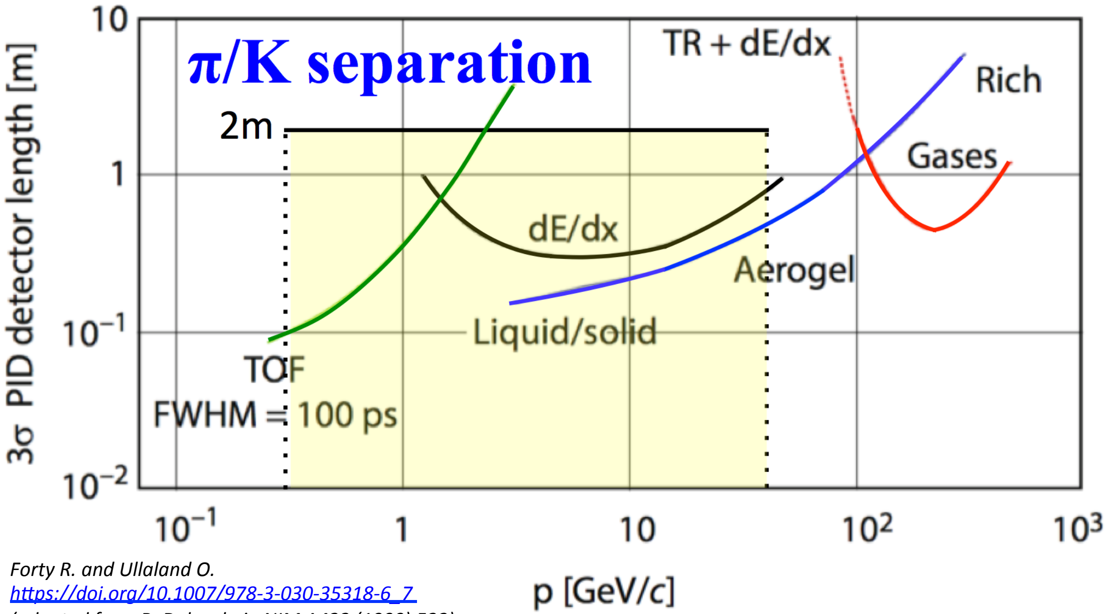

Forty R. and Ullaland O.
https://doi.org/10.1007/978-3-030-35318-6_7
(adapted from B. Dolgoshein NIM A433 (1999) 533)

dE/dx

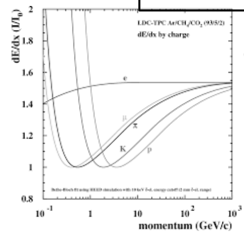

$$-\frac{dE}{dx} = Kz^2\frac{Z}{A}\frac{1}{\beta^2}\left[\ln\frac{2m_ec^2\beta^2\gamma^2T_{max}}{I^2} - \beta^2 - \frac{\delta(\beta\gamma)}{2}\right]$$

$$T_{max} = \frac{2m_ec^2\beta^2\gamma^2}{1+\frac{2\gamma m_e}{M}+\left(\frac{m_e}{M}\right)^2}$$

$$N_{cluster} = \int_0^L \frac{1}{w(x)}\frac{dE}{dx}dx$$

$dN_{cluster}/dx$

$$\Delta t = \frac{L}{c}\left(\frac{1}{\beta_1} - \frac{1}{\beta_2}\right) = \frac{L}{c}\left(\sqrt{1+m_1^2c^2/p^2} - \sqrt{1+m_2^2c^2/p^2}\right) \approx \frac{Lc}{2p^2}\left(m_1^2 - m_2^2\right)$$

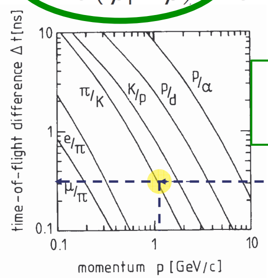

Δt for L = 1 m path length

TOF

σ_t = 300 ps
π/K separation up to 1 GeV/c

$$\cos\theta_c = \frac{1}{n\beta}$$

Rich

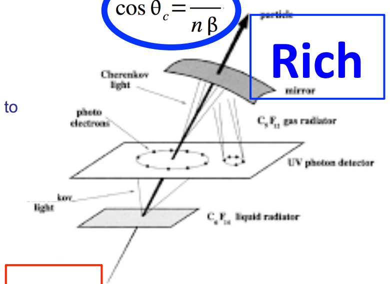

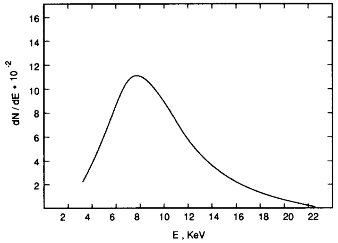

TR

$$W = \frac{1}{3}\alpha\hbar\omega_p\gamma$$

$$\omega_p = \sqrt{\frac{N_e e^2}{\epsilon_0 m_e}} \qquad \hbar\omega_p = 20\,eV$$

PId with dE/dx: the task

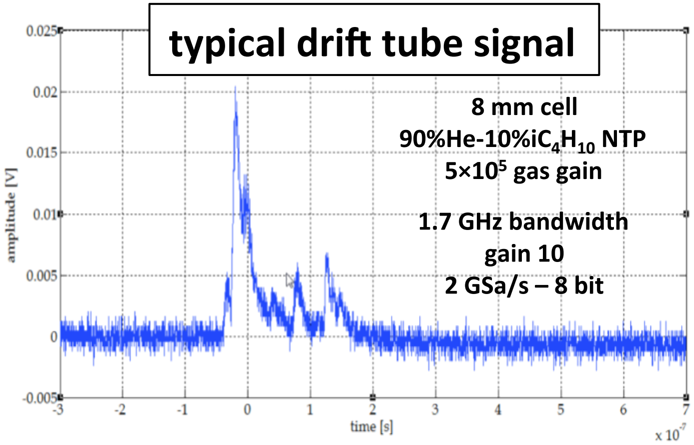

By definition, **the integral** of this signal is proportional to the **total number of electrons** liberated in the ionization process which, in turn, is proportional to the **energy lost** by the charged particle crossing the **x** layer of gas (**-dE/dx**). Knowing the dependence of dE/dx form the velocity **β** of the crossing particle, given **p**, one can identify the particle **mass**.

Also, the **theory model description of the energy loss mechanism** needs to be accurate **at 1% level**

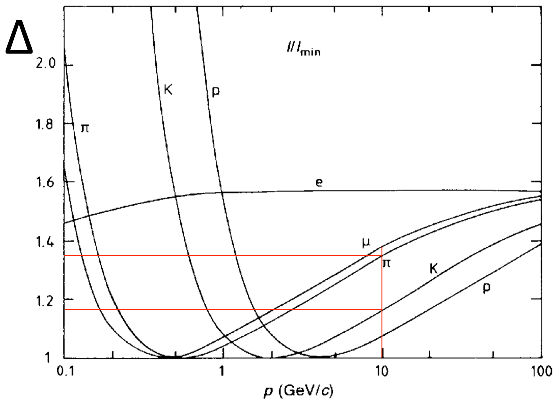

In the relativistic rise region:
[Δ(π) – Δ(K)] / Δ(π) ≈ 10-15%
π/K separation requires
resolutions δΔ/Δ
of **better than a few %**

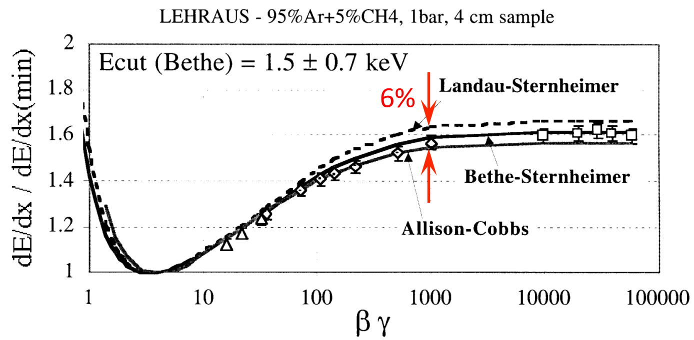

many accurate comparisons here

J. Va'vra
Particle Identification Methods in High Energy Physics,
SLAC-PUB-8356, Jan. 2000

PId with dE/dx: the straggling function

Definitions and iterative application of convolution integral

$\mathbf{d\sigma(E,\beta)/dE}$ collision cross section for an energy transfer **E** by a particle of velocity $\boldsymbol{\beta}$

$\boldsymbol{\lambda = \lambda(\beta) = 1/(n_e\sigma)}$ mean free path between collisions ($\mathbf{n_e}$ = linear density of electrons)

$\mathbf{N_c = x/\lambda}$ mean number of collisions over a length **x**

$$F_{(1)}(E) = 1/\sigma \, d\sigma(E,\beta)/dE = n_e\lambda \, d\sigma(E,\beta)/dE$$

probability to transfer energy **E** in a single collision

$$F_{(k)}(\Delta) = \int_0^{\Delta} F_{(1)}(E)\, F_{(k-1)}(\Delta-E)\, dE$$

probability to transfer energy **Δ** in **k** collisions

k-fold convolution of $\mathbf{F_{(1)}(E)}$

$$P(k, N_c) = N_c^{\,k}/k! \exp(-N_c)$$

probability of **k** collisions with mean $\mathbf{N_c}$ (Poisson)

$$f(\Delta,x) = \sum_{k=0}^{\infty} P(k, N_c)\, F_{(k)}(\Delta)$$

probability density function for energy loss **Δ** over **x**

(straggling function)

[Bichsel et al., Phys. Rev. A 11, 1286 (1975)]

PId with dE/dx: the straggling function

convolution method

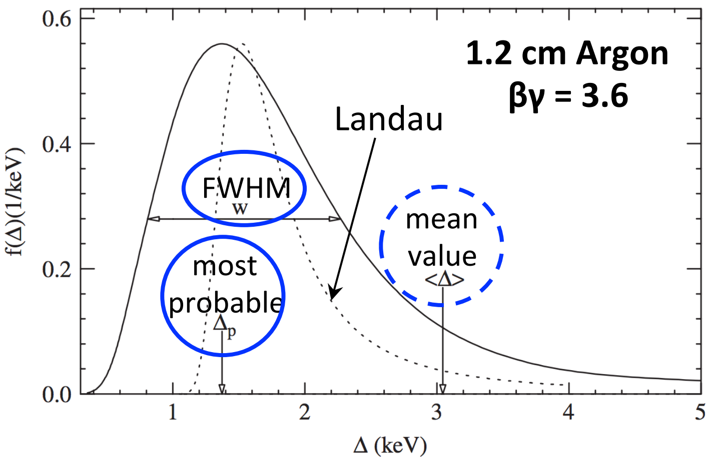

Fig. 1. The straggling function $f(\Delta)$ for particles with $\beta\gamma = 3.6$ traversing 1.2 cm of Ar gas is given by the solid line. It extends beyond $E_{max} \sim 2\,mc^2\beta^2\gamma^2 = 13$ MeV. The original Landau function [2,3] is given by the dotted line. Parameters describing $f(\Delta)$ are the most probable energy loss $\Delta_p(x;\beta\gamma)$, i.e. the position of the maximum of the straggling function, at 1371 eV, and the full-width-at-half-maximum (FWHM) $w(x;\beta\gamma) = 1463$ eV. The mean energy loss is $\langle\Delta\rangle = 3044$ eV.

parameters describing the straggling function:

most probable energy loss **$\Delta_p(x,\beta\gamma)$**

and

FWHM **$W(x,\beta\gamma)$**

There exist several different approaches to calculate the energy loss distribution (**the straggling function**) besides the convolution method (iterative application of convolution integral):

- **Laplace transform** method*
- **Monte Carlo method****
- **empirical fit to data*****

and a plethora of different models based on different parameterization of the collision cross section **σ** with *ad-hoc* corrections

for a rigorous treatment see:

H. Bichsel
A method to improve tracking and particle identification in TPCs and silicon detectors
NIM A562 (2006) 154

*L. Landau, J. Phys. USSR 8, 201 (1944)
**Cobb et al., Nucl. Instr. Meth. 133, 315 (1976)
***Blum, Riegler, Rolandi, Springer-Verlag 2008
doi: 10.1007/978-3-540-76684-1 10

PId with dE/dx: the straggling function

comparison with data

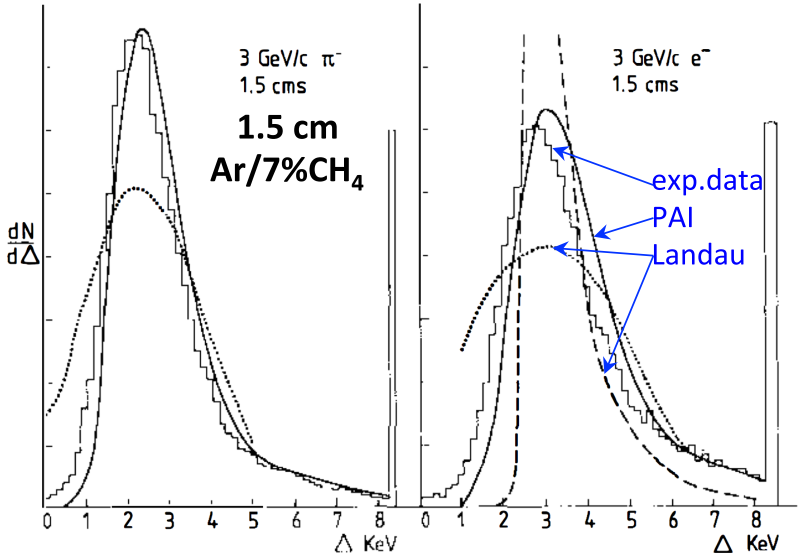

Figure 9 Experimental energy-loss distributions of Harris et al (1973) for π and e at 3 GeV/c in 1.5 cm of argon/7% CH_4 at normal density. The dashed and dotted curves are calculations using the model of Landau (1944) with corrections of Maccabee & Papworth (1969) and Blunck & Leisegang (1950) respectively. The solid curves are the predictions of the PAI model.

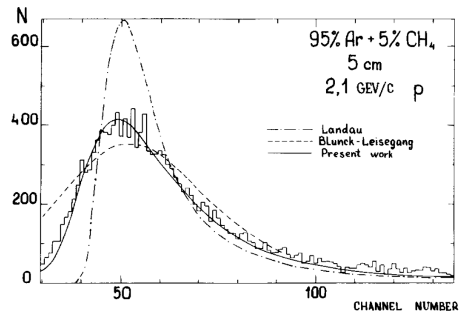

Fig. 4. The energy loss distributions for 2.1 GeV/c protons (near ionization minimum) in 5 cm of a mixture of Ar (95%) and CH_4 (5%). The histogram is obtained in the experiment by Kopot et al.[13]). The smooth curves are calculated for 5 cm of Ar at NTP without correction for detector resolution. The dash–dotted, dashed and solid curves are Landau, Blunck–Leisegang distributions and present work results respectively. Experimental and calculated data are normalised to the same Δ_{mp}.

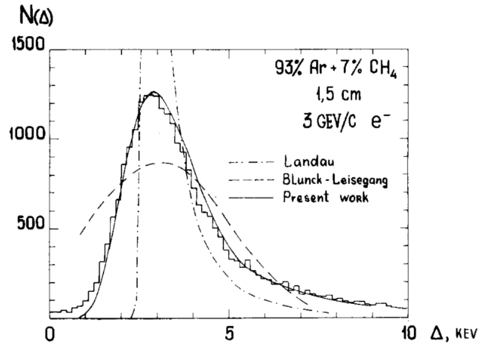

Fig. 5. The energy loss distribution for 3 GeV/c electrons (Fermi plateau region) in 1.5 cm of a mixture of Ar (93%) and CH_4(7%). The histogram is taken from a paper by Harris et al.[9]). The smooth curves are calculated for 1.5 cm of Ar at NTP without correction for detector resolution. The dash–dotted, dashed and solid curves are Landau, Blunck–Leisegang predictions and present work results respectively.

W. Allison and J. Cobb
Relativistic charged particles identification by energy loss
Ann. Rev. Nucl. Part. Sci. 1980. 30: 253-98

V. Ermilova, L. Kotenko, G. Merzon
Fluctuations and the most probable values of relativistic charged particle energy loss in thin gas layers
NIM 145 (1977) 555

PId with dE/dx: the maximum likelihood measurement

- The energy loss distribution (straggling function) **f(Δ)** for a single sample is made of **a broad peak** due to low energy transfer (**soft**) **collisions** with the gas molecules and **a long tail** due to large energy transfer (**hard**) **collisions** which cause the release of **more than one electron** and/or **δ rays**.

- Typical **FWHM** of the energy loss distribution is in the range of **60-100%** $\boldsymbol{\Delta_p}$ (very slowly dependent from βγ – except for very small sample lengths), which makes necessary to measure many samples (**n**) along the ionizing track in order to get a good enough estimate of the energy loss.

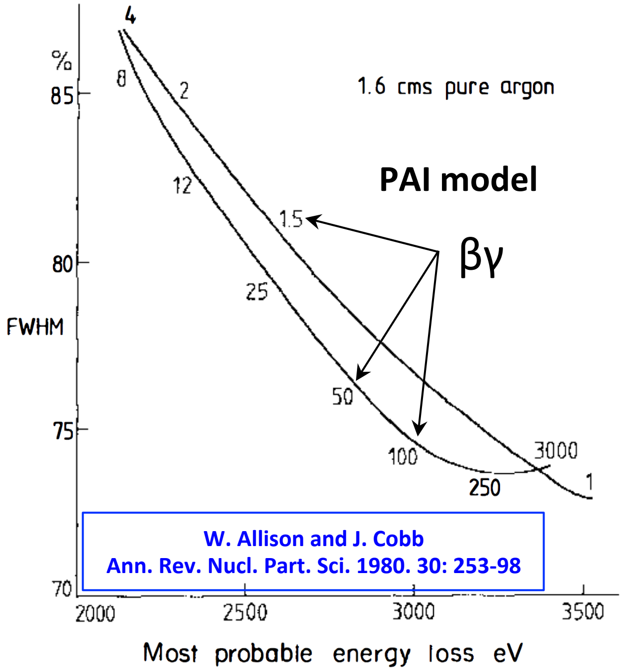

- With the assumption that the shape of the straggling function doesn't depend on βγ, one can construct a **likelihood function**:

$$\mathbf{L(\lambda) = \prod_{i=1}^{n} f(\Delta_i/\lambda).}$$

The $\boldsymbol{\lambda_0}$ (with its error $\boldsymbol{\delta(\lambda_0)}$) which maximizes **L(λ)** is normally distributed and represents **the measured value of the most probable energy loss by the track under scrutiny**.
The mass assignment may then be calculated by comparing the expected ionization with $\boldsymbol{\lambda_0}$ and $\boldsymbol{\delta(\lambda_0)}$ using **normal error statistics**.

PId with dE/dx: the truncated mean measurement

- A much simpler and more robust procedure for obtaining analogous results is the method of **truncated mean**.
- It consists in cutting out a fraction **$(1-\eta)\cdot n$** of the largest Δ_i samples and extending the arithmetic mean to the remaining **$\eta\cdot n$** values (**m** is the closest integer to $\eta\cdot n$):

$$<\Delta>_\eta = 1/m \sum_{j=1}^{m} \Delta_j \qquad \Delta_j \leq \Delta_{j+1} \quad \text{for } j = 1, \ldots, n-1$$

- It can be shown that the range of values of **η** which minimizes the relative fluctuations of **$<\Delta>_\eta$** for **Argon** is **between 0.4 and 0.7** (**0.8 for Helium**). Moreover, the **$<\Delta>_\eta$** distribution behaves like a **gaussian distribution.**
- This is equivalent to the maximum likelihood method with:

$$<\Delta>_\eta \cong \lambda_0 \quad \text{and} \quad \sigma(<\Delta>_\eta) \cong \delta(\lambda_0)$$

PId with dE/dx: alternative methods?

Besides the truncated arithmetic mean, are there other effective methods?

data from BES III

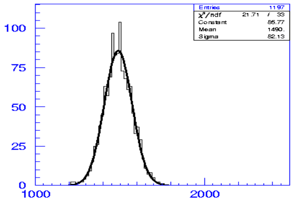

dE/dx of truncated mean

TM 70%

σ = 5.51%

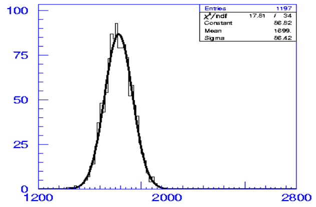

dE/dx of geometric mean

$$< \Delta >_g = \sqrt[n]{\prod_{i=1}^{n} \Delta_i}$$

σ = 5.09%

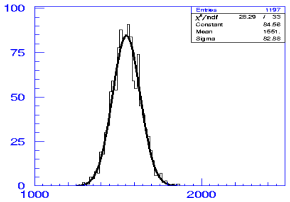

dE/dx of double truncated mean

2TM 5-75%

σ = 5.34%

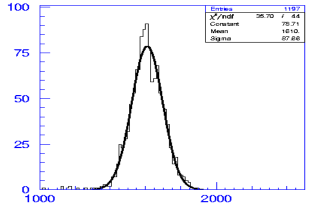

dE/dx of harmonic mean

$$< \Delta >_h = \frac{n}{\sum_{i=1}^{n} 1/\Delta_i}$$

σ = 5.44%

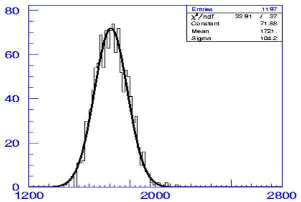

dE/dx of median

σ = 6.06%

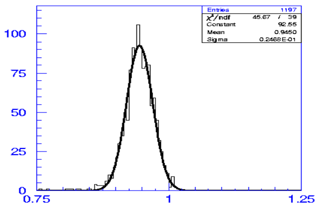

dE/dx of transformed mean

$$< \Delta >_t = \left(\sum_{i=1}^{n} \frac{1}{\sqrt{\Delta_i}} \right)^{-1}$$

σ = 2.61%

M. Hauschild
Progress in dE/dx techniques used for particle identification
NIM A379(1996) 436

PId with dE/dx: particle separation power

✧ The relevant quantity for discriminating between two different particle of masses **1** and **2** of momentum **p**, rather than $\boldsymbol{\lambda_0}$ and $\boldsymbol{\delta(\lambda_0)}$ for each of them, is:

$$D_{12}(p) = \frac{|\lambda_{0,1}(p) - \lambda_{0,2}(p)|}{[\sigma(\lambda_{0,1}) + \sigma(\lambda_{0,2})]/2}$$

(separation measured in number of sigma $\boldsymbol{\sigma(\lambda_0) = \delta(\lambda_0)/\lambda_0}$)

ALEPH TPC

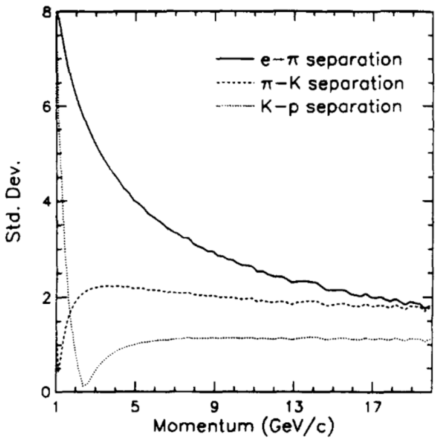

two-sided truncated mean: discard lowest 8% and largest 40%

$$\frac{\sigma_{dE/dx}}{(dE/dx)} = 4.5\%$$

OPAL Drift Chamber (4 bar)

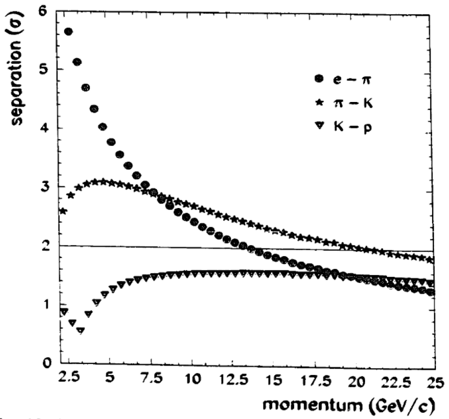

hit quality cuts and truncated mean: discard largest 30%

$$\frac{\sigma_{dE/dx}}{(dE/dx)} = \begin{matrix} 3.1\% \text{ (dimuons)} \\ 3.8\% \text{ (m.i.p.)} \end{matrix}$$

PId with dE/dx: a few experimental facts for a PId detector

✧ Number of ionization acts follows **Poison distribution** (≈10/cm/bar for He based, ≈30/cm/bar for Ar based gas mixtures)

✧ Number of electrons generated in each ionization act (**cluster size**) is subject to large fluctuations (slide)

✧ The accuracy of the ionization measurement depends on the mean free path between ionizing collisions $\boldsymbol{\lambda = 1/(n_e\sigma)}$ (i.e., on the collision cross section $\boldsymbol{\sigma}$ and on the electron number density $\mathbf{n_e}$), therefore, on

- the **gas** mixture;
- the **sample length x** and its density, or the **gas pressure p** through their product **xp**;
- the number of samples **n**, or, equivalently, the total length of the track **L = nx**.

✧ Empirical parameterization of resolution $\sigma(\lambda_0) = \delta(\lambda_0)/\lambda_0$ ([%] xp in [cm bar]) (slide):

$$\boldsymbol{\sigma(\lambda_0) = 41\, n^{-0.46}\, (xp)^{-0.32}\ [\%]}$$ (based on max. likel., −0.46 → −0.43 with trunc. mean)

for Argon Allison-Cobb Walenta

✧ Number of electrons generated per cluster subject to large fluctuations

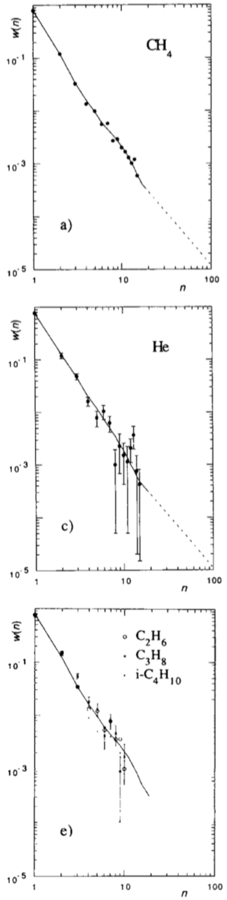

H. Fischle, J. Heintze and B. Schmidt, *Experimental determination of ionization cluster size distributions in counting gases,* **NIM A 301 (1991)**

	CH_4	Ar	He	CO_2
k				
1	78.6	65.6	76.60	72.50
2	12.0	15.0	12.50	14.00
3	3.4	6.4	4.60	4.20
4	1.6	3.5	2.0	2.20
5	0.95	2.25	1.2	1.40
6	0.60	1.55	0.75	1.00
7	0.44	1.05	0.50	0.75
8	0.34	0.81	0.36	0.55
9	0.27	0.61	0.25	0.46
10	0.21	0.49	0.19	0.38
11	0.17	0.39	0.14	0.34
12	0.13	0.30	0.10	0.28
13	0.10	0.25	0.08	0.24
14	0.08	0.20	0.06	0.20
15	0.06	0.16	0.048	0.16
16	(0.050)	0.12	(0.043)	0.12
17	(0.042)	0.095	(0.038)	0.09
18	(0.037)	0.075	(0.034)	(0.064)
19	(0.033)	(0.063)	(0.030)	(0.048)
$\geq$20	$(11.9/k^2)$	$(21.6/k^2)$	$(10.9/k^2)$	$(14.9/k^2)$

HEED simulation
1 cm
He/iC_4H_{10} - 90/10

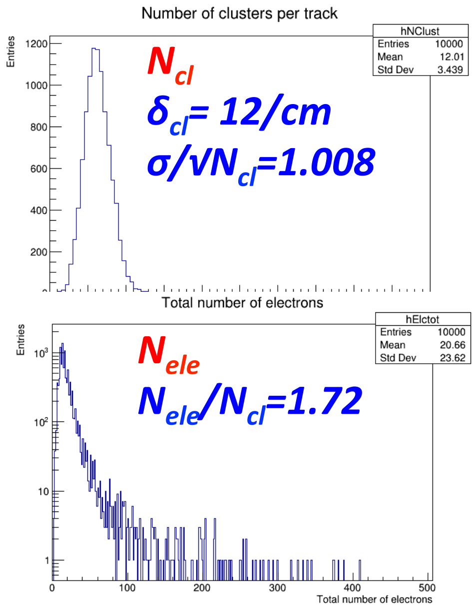

F. Cuna, G. Tassielli *private communication*

notice the steeper distribution for **He** with respect to **Ar**

✧ Parameterization of resolution $\sigma(\lambda_0)$

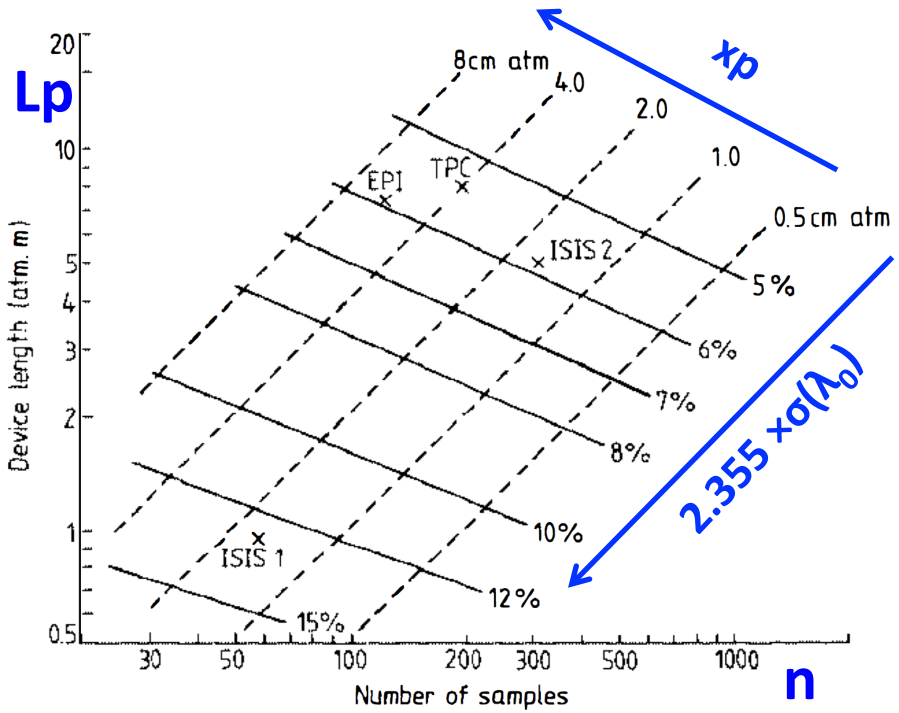

W. Allison and J. Cobb
Relativistic charged particles identification by energy loss
Ann. Rev. Nucl. Part. Sci. 1980. 30: 253-98

- keeping x fixed and increasing n or L improves the resolution
- keeping n fixed and varying L and x improves the resolution (slide)
- what is the optimal sample length for a fixed total length L?

  the finer the better **($n^{-0.14}$)**

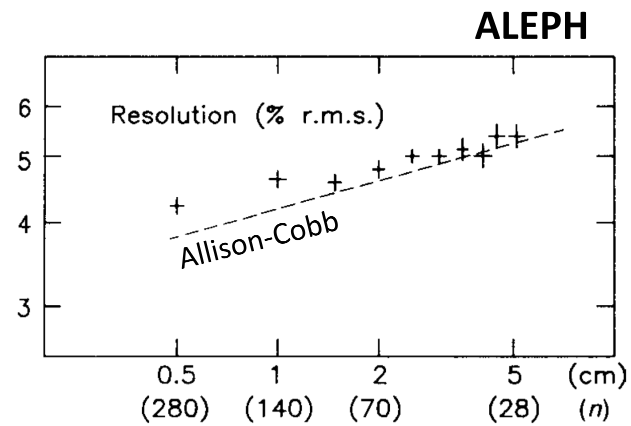

✧ Average number of electrons per cluster increases with sample length

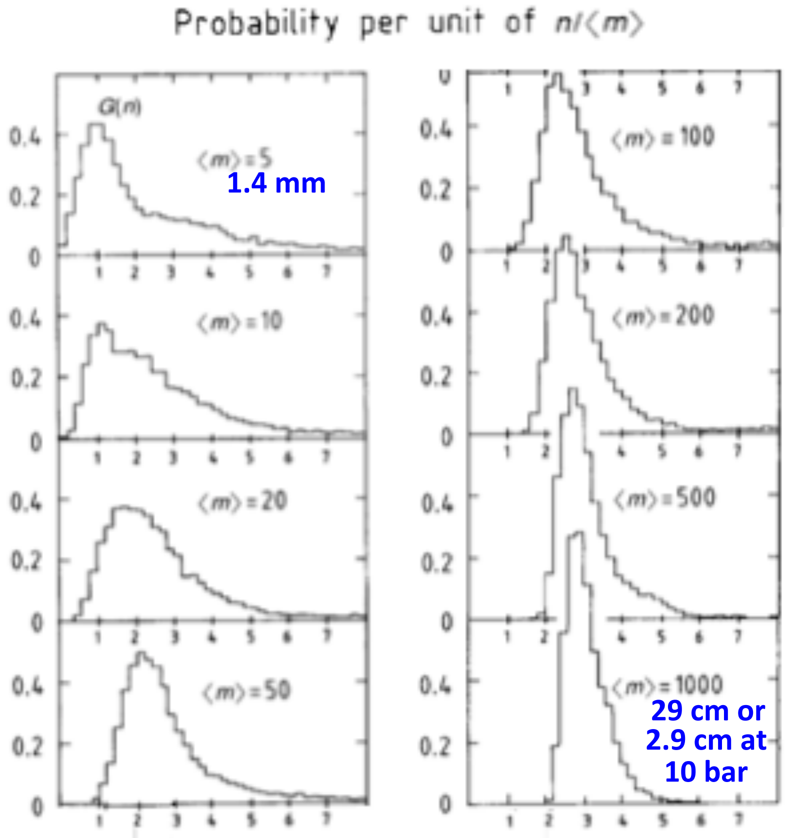

cluster size - Ar based gas

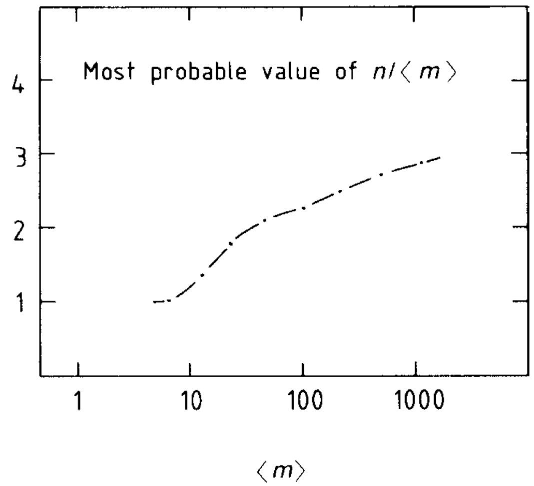

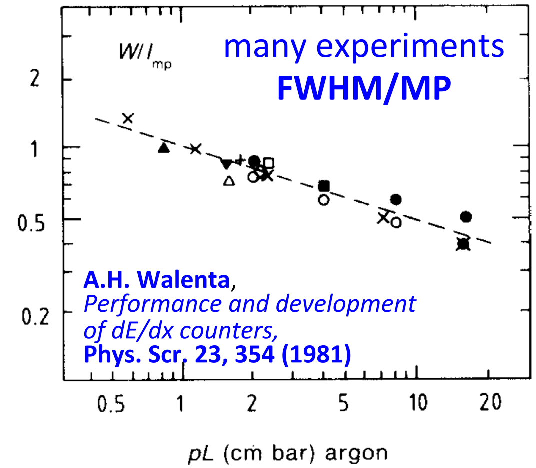

PId with dE/dx: gas choice

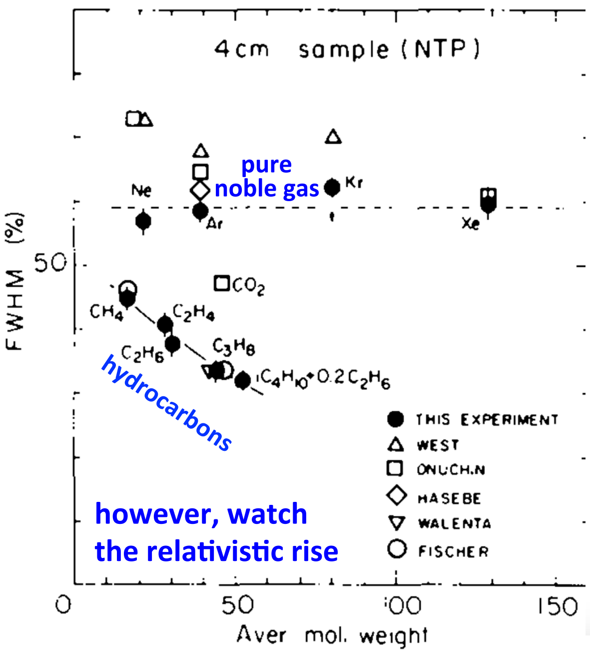

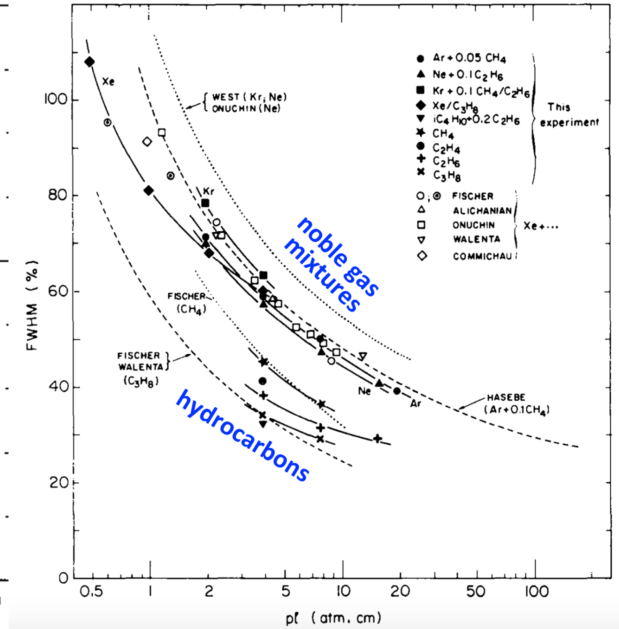

I. Lehraus, R. Mattewson and W. Tejesse, *dE/dx measurements in Ne, Ar, Kr, Xe and pure hydrocarbons,* **NIM 200 (1982) 199**

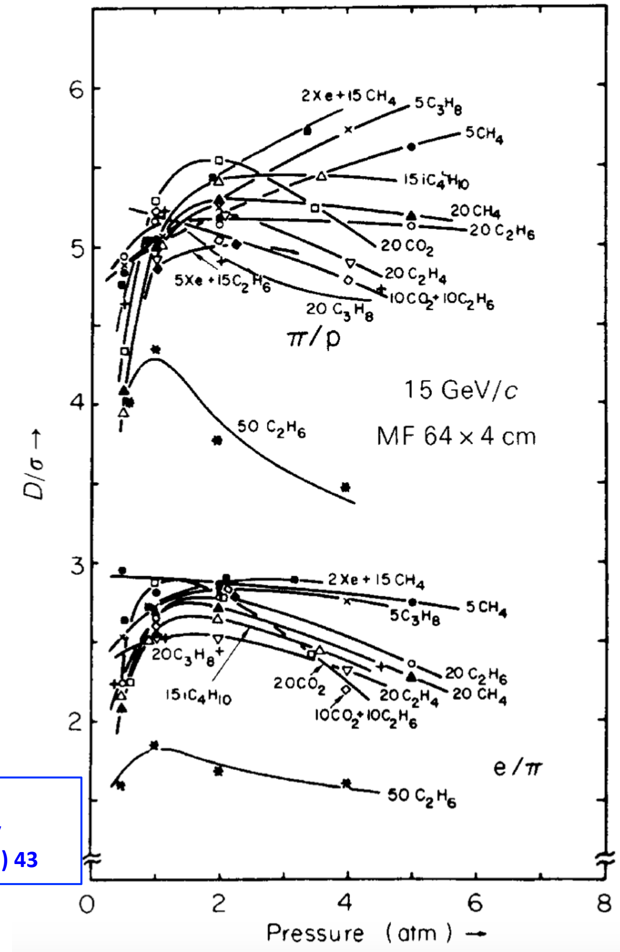

I. Lehraus, *Progress in particle identification by ionization sampling,* **NIM 217 (1983) 43**

dE/dx performance

Detector	Accelerator	Type	Size (Ø x L)	B (T)	Gas Mixture	Pressure (bar)	Number of samples	Sampling length (mm)	Effective track length (bar * m)	dE/dx resolution isol. (%)	dE/dx resolution dense (%)	Truncations (%)	Reference		
ALEPH	LEP	TPC	3.6 m x 4.4 m	1.5	Ar/CH_4 (91/9)	1	338	4	1.35	4.5		8-60	D. Buskulic et al., NIM A 360 (1995) 481		
ARGUS	DORIS	drift cells	1.7 m x 2 m	0.8	C_3H_8/Methylal	1	36	18	0.65	4.1	(4.4)	10-70	Y. Oku, PhD Thesis, Univ. of Lund (1985), LUNFD6/(NFFL-7024)/		
BaBar	PEP-II	drift cells	1.6 m x 2.8 m	1.5	$He/i\text{-}C_4H_{10}$ (80/20)	1	40	12	0.48	7.5		0-80	B. Aubert et al., NIM A 479 (2002) 1-116	7.1	-7%
BELLE	KEK-B	drift cells	1.9 m x 2.2 m	1.5	He/C_2H_6 (50/50)	1	47	16	0.75	5.5	(7.0)	0-80	E. Nakano, NIM A 494 (2002) 402-408	6.0	+9%
BES	BEPC	jet cells	2.3 m x 2.1 m	0.4	$Ar/CO_2/CH_4$ (89/10/1)	1	54	5	0.27	9.0		0-70	J.Z. Bai et al., NIM A 344 (1994) 319		
CDF	TEVATRON	jet cells	2.6 m x 3.2 m	1.5	$Ar/C_2H_6/C_2H_6O$ (49.6/49.6/0.8)	1	32	12	0.38	7.0		?	D. Stuart, private communications		
CLEO II	CESR	drift cells	1.9 m x 1.9 m	1.5	Ar/C_2H_6 (50/50)	1	51	14	0.71	6.2	(7.1)	0-50	Y. Kubota et al., NIM A 320 (1992) 66		
CLEO III	CESR	drift cells	1.6 m x 1.9 m	1.5	He/C_3H_8 (60/40)	1	47	14	0.66	5.0		0-70	D. Peterson et al., NIM A 478 (2002) 142-146	6.3	+26%
CRISIS	TEVATRON	jet cells	1 m x 1 m x 3 m	-	Ar/CO_2 (80/20)	1	192	15	2.88	3.2		0-75	W.S. Toothacker et al., NIM A 273 (1988) 97	3.2	0%
DELPHI	LEP	TPC	2.4 m x 2.7 m	1.2	Ar/CH_4 (80/20)	1	192	4	0.77	5.7	(6.2)	0-80	P. Abreu et. al., CERN-PPE/95-194, submitted to NIM		
D0 FDC	TEVATRON	jet cells	1.2 m x 0.3 m	-	$Ar/CH_4/CO_2$ (93/4/3)	1	32	8	0.26	12.7		0-70	S. Rajagopalan, PhD Thesis, Northwestern University (1992)		
H1	HERA	jet cells	1.7 m x 2.2 m	1.13	Ar/C_2H_6 (50/50)	1	56	10	0.56	10.0		none*	I. Abt et al., NIM A 386 (1997) 348-396		
JADE	PETRA	jet cells	1.6 m x 2.4 m	0.48	$Ar/CH_4/i\text{-}C_4H_{10}$ (88.7/8.5/2.8)	4	48	10	1.92	6.5	(7.2)	5-70	K. Ambrus, PhD Thesis, Univ. of Heidelberg (1986)		
KEDR	VEPP-4M	jet cells	1.1 m x 1.1 m	2.0	DME (100)	1	42	10	0.42	10.0		5-70	S.E. Baru et al., NIM A 323 (1992) 151		
KLOE	DAΦNE	drift cells	4 m x 3.3 m	0.6	$He/i\text{-}C_4H_{10}$ (90/10)	1	58	28	1.62	3.5		0-80	A. Andryakov et al., NIM A 409 (1998) 390-394 (prototype)	4.5	+28%
MARK II	SLC	drift cells	3 m x 2.3 m	0.475	$Ar/CO_2/CH_4$ (89/10/1)	1	72	8.33	0.60	7.0		5-75	A. Bojarski et al., NIM A 283 (1989) 617		
NA49	SPS	TPC	3.8 m x 3.8 m x 1.3 m	-	$Ar/CH_4/CO_2$ (90/5/5)	1	90	40	3.60	4.7		10-65	B. Lasiuk, NIM A 409 (1998) 402-406		
OBELIX	LEAR	jet cells	1.6 m x 1.4 m	0.5	Ar/C_2H_6 (50/50)	1	40	15	0.60	12.0		0-70	F. Balestra et al., NIM A 323 (1992) 523		
OPAL	LEP	jet cells	3.6 m x 4 m	0.435	$Ar/CH_4/i\text{-}C_4H_{10}$ (88.2/9.8/2)	4	159	10	6.36	2.8	(3.2)	0-70	M. Hauschild, NIM A 379 (1996) 436.	2.6	-7%
SLD	SLC	jet cells	2 m x 2 m	0.6	$CO_2/Ar/i\text{-}C_4H_{10}$ (75/21/4)	1	80	6	0.48	7.0		?	M. Hildreth, private communications		
STAR	RHIC	TPC	4 m x 4.2 m	0.5	Ar/CH_4 (90/10)	1	45	17.2	0.77	8.0		0-70	M. Anderson et al., NIM A xxx (2003), in print		
TOPAZ	TRISTAN	TPC	2.4 m x 2.2 m	1.0	Ar/CH_4 (90/10)	3.5	175	4	2.45	4.4	(4.6)	0-65	M. Iwasaki et al., NIM A 365 (1995) 143		
TPC/2γ	PEP	TPC	2 m x 2 m	1.375	Ar/CH_4 (80/20)	8.5	183	4	6.22	3.0		0-65	G. Cowan, PhD Thesis, Lawrence Berkeley Lab. (1988), LBL-24715	2.5	-17%
ZEUS	HERA	jet cells	1.7 m x 2.4 m	1.43	$Ar/CO_2/C_2H_6$ (90/8/2)	1	72	8	0.58	8.5		?	W. Zeuner, private communications		

best performance

He based gas

* = inverse gaussian mean 1/sqrt[(dE/dx)i] used

Particle Identification Techniques with dE/dx

Michael Hauschild, 8th ICATPP, Como, 8-Oct-2003, page 26

Factors affecting uniform track signal response

W. Allison and P. Wright
The Physics of Charged Particle Identification
OUNP 35-83

Gas related factors

- composition (stability, pollutants)
- environmental parameters (pressure, temperature, ...)
- drift, gas gain, diffusion, space charge, attenuation

Geometry factors

- track angle
- cell geometry
- mechanical tolerances
- field uniformity

Electronics factors

- noise (white)
- coherent noise
- baseline stability
- threshold stability
- bandwidth
- electronic gain uniformity (calibrations)

dE/dx comments and summary

- ✧ Methodology dating back to '80s. Very little progress in performance since then.
- ✧ Helium based gas mixtures, a priori disfavored because of the lower ionization statistics, compensate with fewer fluctuations and equal the Argon performance.
- ✧ However, much less documentation exists for dE/dx with Helium mixtures.
- ✧ Using the Allison-Cobb parameterization a **dE/dx resolution between 4.0% and 4.5%** is granted
- ✧ Given the very low He density, an increase in pressure might improve separation power (by 20% at 2 bar) without jeopardizing too much the momentum resolution (special PId dedicated runs?).
- ✧ A further 25% improvement may come at the expensive cost of a finer (×2) drift cell granularity.
- ✧ New techniques (ML?) might make the difference with respect to maximum likelihood and/or truncated mean methods, but do not expect miracles.
- ✧ Only a completely different approach, **cluster counting**, may provide the necessary quantum leap.

PId with dN/dx: the task

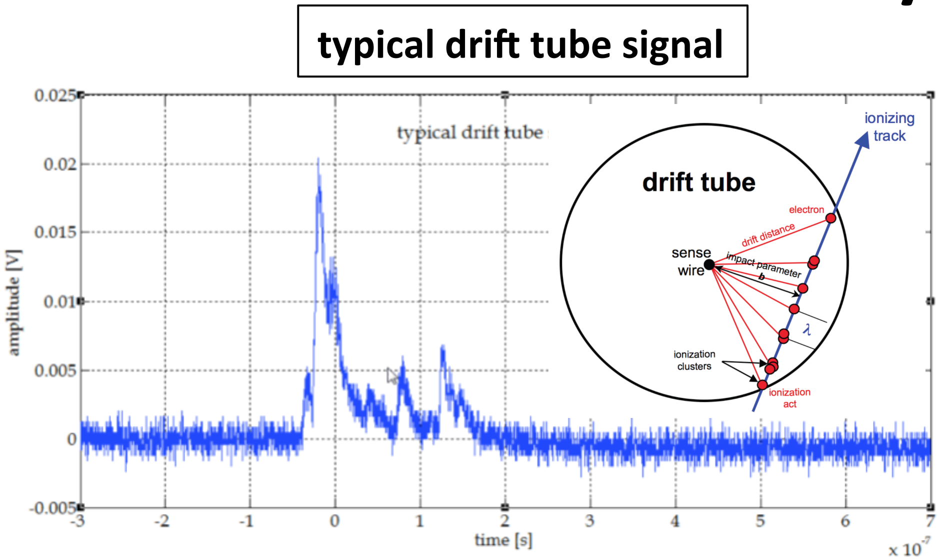

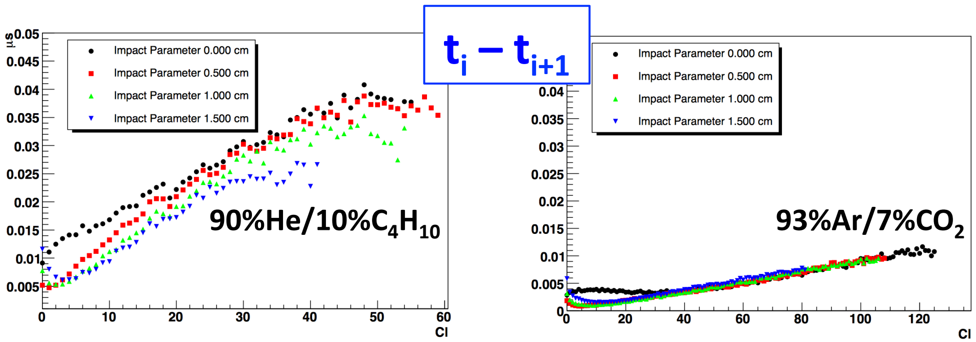

- **Cluster counting** consists in singling out, in every recorded detector signal, **the isolated structures related to the arrival at the anode wire of the electrons belonging to a single ionization act**.
- In order to achieve this goal, special experimental conditions must be met**: pulses from electrons belonging to different clusters must have a little chance of overlapping in time** and, at the same time, **the time distance between pulses generated by electrons coming from the same cluster must be small enough to prevent over-counting**.
- The fulfillment of both these requirements involves incompatible time resolutions: it appears that **the optimal counting condition can be reached only as a result of the equilibrium** between the fluctuations of those processes which forbid a **full cluster detection efficiency** and of the ones enhancing the **time separation among different ionization events**.

PId with dN/dx: the task - first approach

- The relevant parameters for a cluster counting measurement are **the resolving time τ** and **the single electron diffusion σ_D**.
- The ideal conditions, which guarantee a real Poisson distribution of the cluster counting, are met with a resolving time **$\tau = 0$**, in absence of diffusion, **$\sigma_D = 0$**.
- For the 90%He/10%C_4H_{10} gas mixture and a 2.5 cm drift cell, the real optimal conditions are met with **$\tau = 4$ ns**
- It should be stressed that the obtained result is strictly related to the **detector geometry** as it depends on the impact parameter and on the dimension of the drift cell for the given gas.
- Corrections due to the track angle, impact parameter, saturation effects, attachment (for long drift) are necessary

impact parameter dependence for 90%He/10%C_4H_{10} 12 clusters/cm

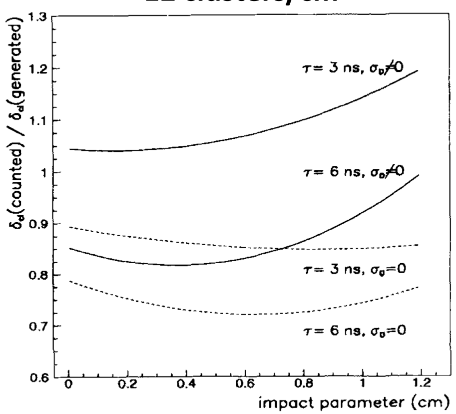

Monte Carlo simulations

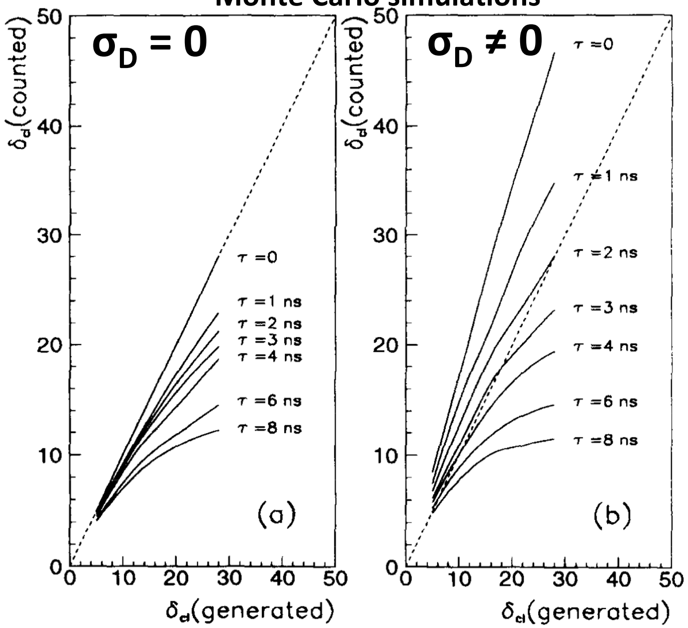

G. Cataldi, F. Grancagnolo, S. Spagnolo
Cluster counting in helium based gas mixtures
NIM A386 (1997) 458

PId with dN/dx: the task – second approach

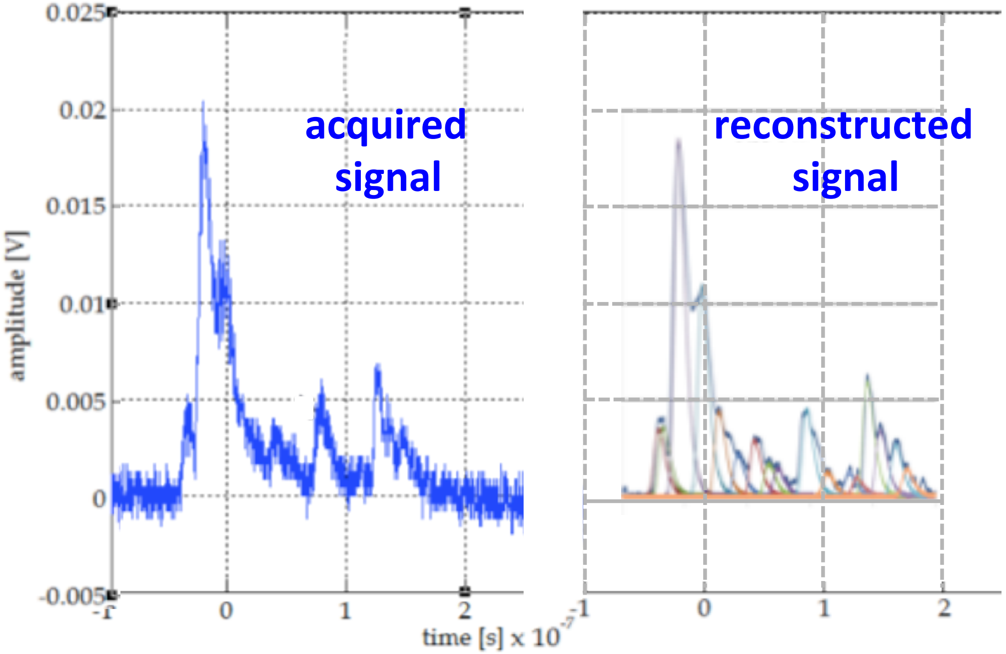

For any given first cluster (**FC**) drift time, the **cluster timing technique** exploits the drift time distribution of all successive clusters to statistically determine, track by track, the most probable **impact parameter**, thus reducing the **bias** and improving the average **spatial resolution** with respect to that obtained from with the FC method alone.

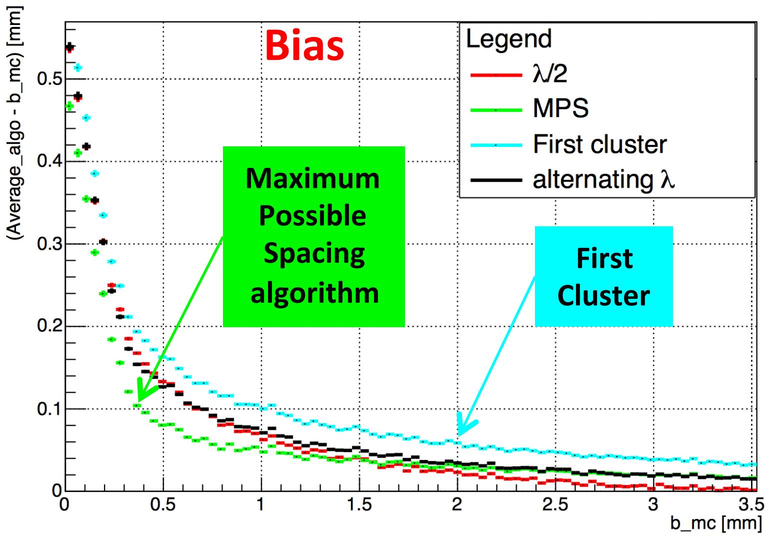

From the **ordered sequence of the electrons arrival times**, considering the average time separation between clusters and their time spread due to diffusion, one can reconstruct **the most probable sequence of clusters drift times** and $\mathbf{N_{cl}}$: $\left\{t_i^{cl}\right\}$, $i = 1, N_{cl}$

dE/dx and dN_{cl}/dx: experimental results

μ/π separation at 200 MeV/c in He/iC_4H_{10} – 95/5 100 samples 3.7 cm

gas gain 2×10^5, 1.7 GHz – gain 10 amplifier, 2GSa/s – 1.1 GHz – 8 bit digitizer

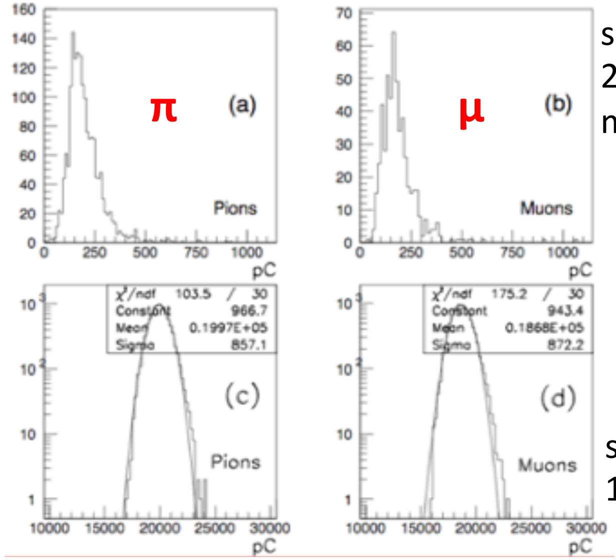

single sample 20% truncated mean

sum over 100 samples

test beam data

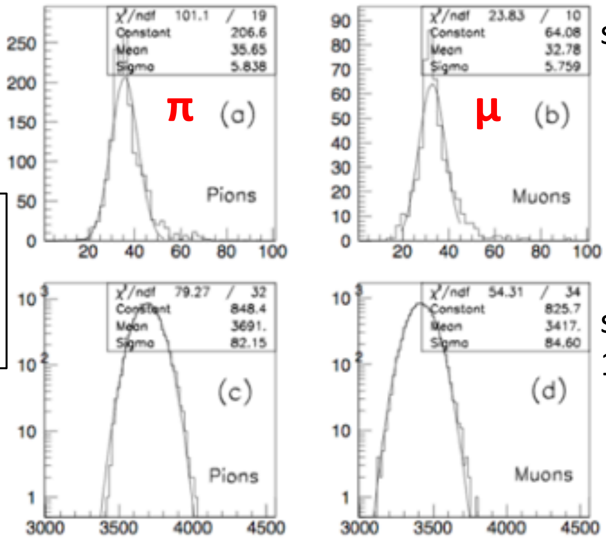

single sample

π: σ/√N_{cl}=0.978
μ: σ/√N_{cl}=1.006

sum over 100 samples

π: σ/√N_{cl}=1.35
μ: σ/√N_{cl}=1.45

integrated charge
expected 2.0 σ separation
measured 1.4 σ separation

cluster counting
expected 5.0 σ separation
measured 3.2 σ separation

G. Cataldi, F. Grancagnolo, S. Spagnolo
Cluster counting in helium based gas mixtures
NIM A386 (1997) 458

dE/dx and dN_{cl}/dx

Expected from analytical calculation for IDEA Drift Chamber

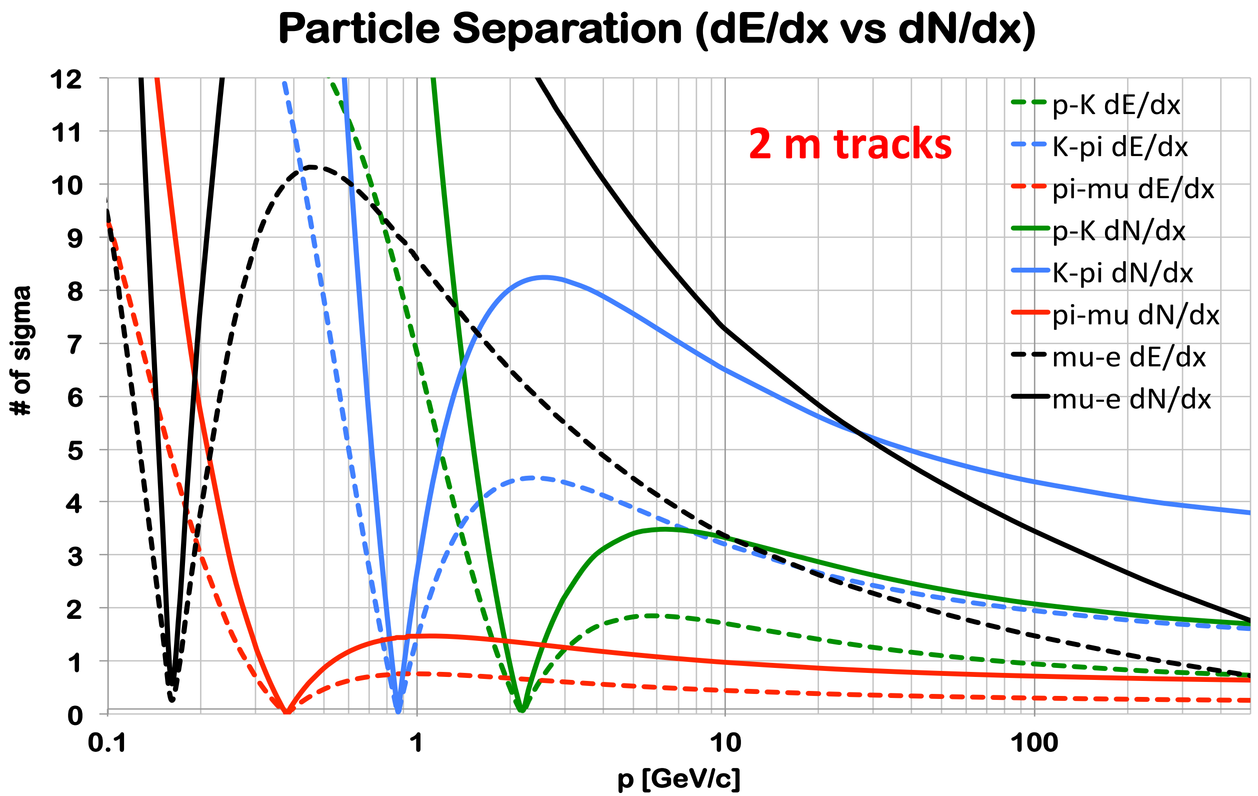

He/iC4H10 90/10

δ_{cl}=12 cm^{-1}

σ(dE/dx)/(dE/dx) =4.3%

80% cluster counting efficiency

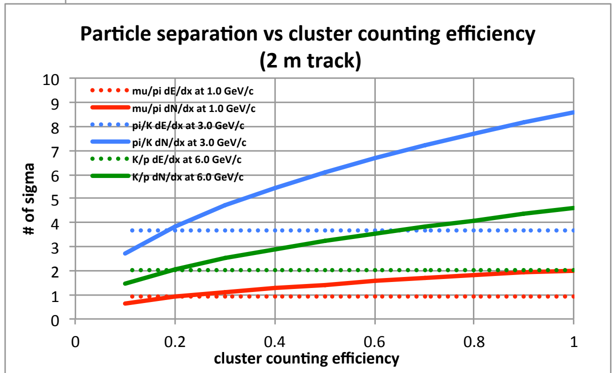

dE/dx and dN_{cl}/dx

Expected from analytical calculation for IDEA Drift Chamber

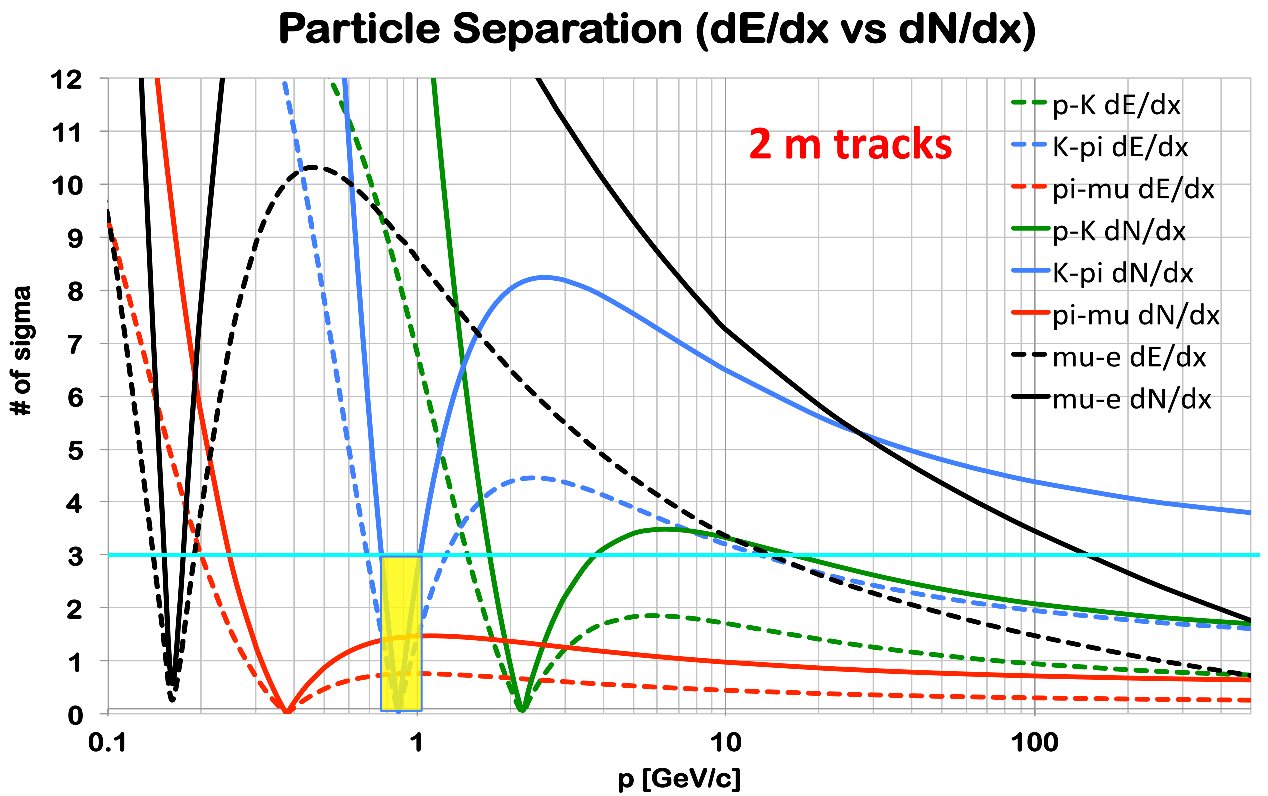

He/iC4H10 90/10

δ_{cl}=12 cm^{-1}

σ(dE/dx)/(dE/dx) =4.3%

80% cluster counting efficiency

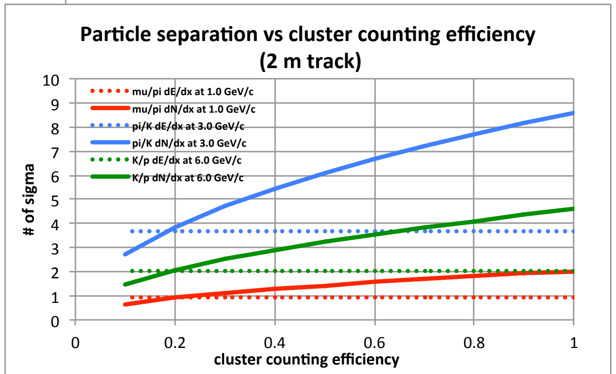

dE/dx and dN_{cl}/dx

Expected from analytical calculation for IDEA Drift Chamber

He/iC4H10 90/10

δ_{cl}=12 cm^{-1}

σ(dE/dx)/(dE/dx)

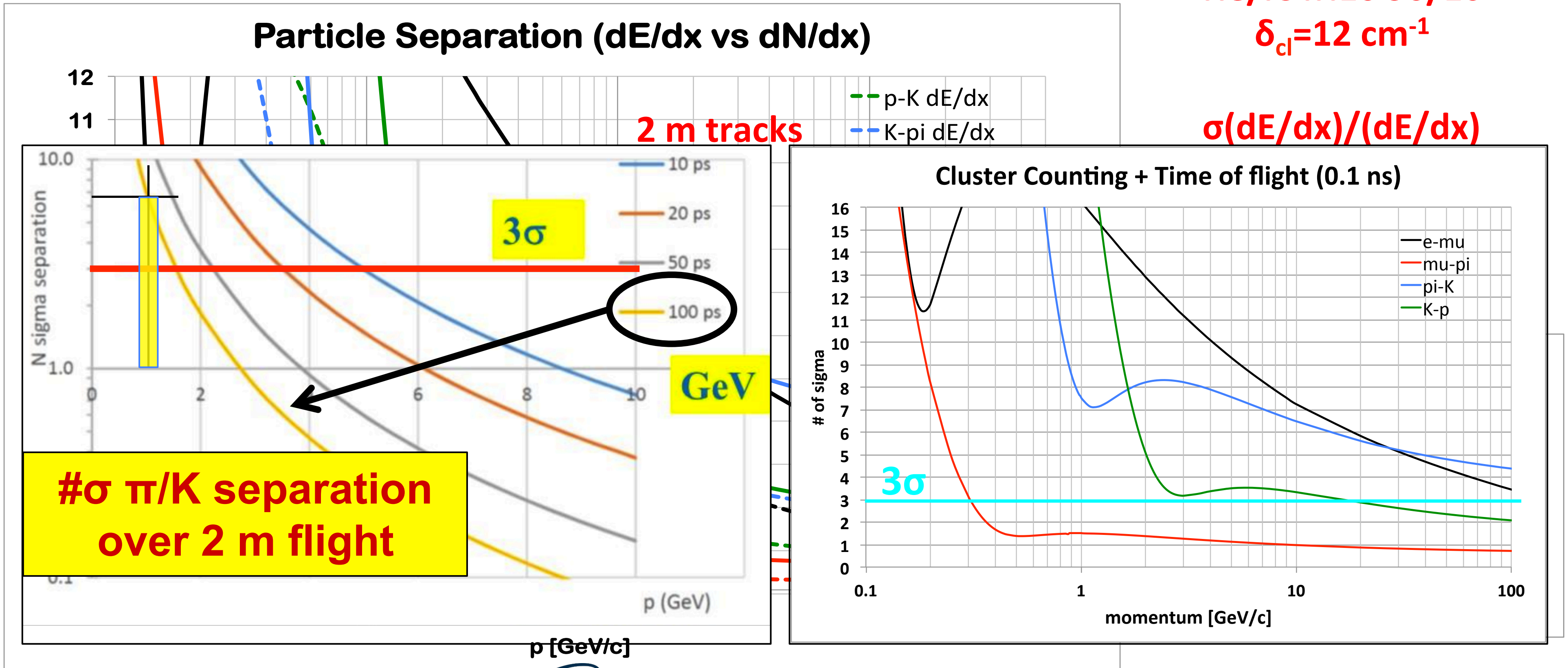

dE/dx and dN_{cl}/dx

Comments:

- PID comes (almost) for free in drift chambers.
- It suffers from blindness at the "crossing points", where additional help is needed
- **dE/dx** resolutions of around 5% are granted, provided high stability is reached on HV and gas parameters and on continuous electronics calibration. Alternatives to the maximum likelihood / truncated mean techniques are highly desirable.
- **dN_{cl}/dx** resolutions are potentially a factor 2 better with respect to dE/dx. Cluster counting requires fast electronics and sophisticated counting algorithms to be fully efficient. However, given its digital nature, it is less dependent on gain stability issues.

$$\boxed{\frac{\sigma_{dE/dx}}{(dE/dx)} = 0.41 \cdot N^{-0.46} \cdot \left(x_{track}[cm] \cdot P[atm]\right)^{-0.32} = 4.4\%}$$

$$\boxed{\frac{\sigma_{dN_{cl}/dx}}{(dN_{cl}/dx)} = \left(\delta_{cl} \cdot L_{track}\right)^{-1/2} = N_{cl}^{-1/2} = 2.2\%}$$

Remarks:

- these techniques require no added complexity (and material!) to the whole detector!
- this is particularly relevant for a high precision EM calorimeter at a few %/sqrt(E)
- no compromise on performance and hermeticity of the detector (control of acceptance required at Z-pole at the level of 10^{-5}!)